Applied Physics Letters

Continuous film spin–orbit torque characterization via four probe measurement

Cite as: Appl. Phys. Lett. **121**, 012405 (2022); https://doi.org/10.1063/5.0092471
Submitted: 23 March 2022 • Accepted: 24 June 2022 • Published Online: 07 July 2022

H. Y. Poh, C. C. I. Ang, T. L. Jin, et al.

Applied Physics Letters ARTICLE scitation.org/journal/apl

Continuous film spin–orbit torque characterization via four probe measurement

Cite as: Appl. Phys. Lett. **121**, 012405 (2022); doi: 10.1063/5.0092471
Submitted: 23 March 2022 · Accepted: 24 June 2022 ·
Published Online: 7 July 2022

H. Y. Poh,[1] C. C. I. Ang,[1] T. L. Jin,[1] F. N. Tan,[1] G. J. Lim,[1] S. Wu,[1] F. Poh,[2] and W. S. Lew[1,a)]

AFFILIATIONS

[1]School of Physical and Mathematical Sciences, Nanyang Technological University, 21 Nanyang Link, Singapore 637371
[2]GLOBALFOUNDRIES Singapore Pte. Ltd., 60 Woodlands Industrial Park D St 2, Singapore 738406

[a)]**Author to whom correspondence should be addressed:** wensiang@ntu.edu.sg

ABSTRACT

Spin–orbit torque (SOT) characterization techniques generally require the Hall cross that generally demands lithography resources and time. It is highly desirable to characterize SOT efficiencies with minimal sample processing time. Here, we demonstrate a lithography-free technique to determine the spin–orbit torque efficiency in a perpendicular magnetic anisotropy ferromagnetic heterostructure. By utilizing a customized four-point probe in a rhombus geometry, harmonic Hall measurement was performed on continuous films of a Pt/Co/Ti structure to characterize the spin–orbit torque efficiency. A correction factor, which is due to the non-uniform current distribution across the continuous film, was experimentally evaluated by taking the ratio of the measured damping-like field of the continuous film to that of a fabricated Hall device. Additionally, this correction factor is analytically derived and experimentally shown to be determined by the configuration of the probes and is independent of the structure material. Our measurement reveals that by performing a single calibration process for the particular set of probes, the same correction factor was validated on a second ferromagnetic heterostructure, Ti/Pt/Co/Ta; hence, it can be applied to other SOT films' stack measurements. Our four-probe harmonic Hall technique provides an alternative and swift way for SOT investigations by eliminating multiple lithography processes necessary in conventional approaches.

The conversion of electrical current to spin current through the spin Hall effect (SHE) has provided an energy-efficient scheme for magnetization manipulation in spintronics devices.[1,2] These spin currents generated by spin–orbit interactions exchange their angular momentum with the ferromagnetic layer's local magnetization, resulting in torque referred to as spin–orbit torque (SOT).[3–6] Under a sufficiently large torque, SOT induces magnetization switching, which is useful for memory storage device writing operations. SOT has drawn much interest due to its fast switching speed and low critical switching current, which offer great potential for applications in spintronics devices.[3,7] Several established experimental techniques to characterize SOT include harmonic Hall measurement, current-induced loop-shifting, and spin–torque ferromagnetic resonance (ST-FMR).[8–12] As an advantageous aspect of harmonic Hall measurement, apart from the easily accessible harmonic Hall measurement technique, the effective SOT field is quantified based on the oscillating Hall voltage perturbation induced by in-plane (IP) alternating currents while under in-plane magnetic fields. The oscillating Hall voltage arises from the SOT-driven magnetization precession about its equilibrium state, allowing for the SOT efficiency quantification. However, this characterization technique, like the other above-mentioned techniques, requires micro- or nanodevice fabrication, involving a series of lithography processes that cost additional resources and time. As the interest in exploring materials for improved SOT performance continues to increase, an efficient technique to characterize SOT efficiencies with minimal processes, equipment, and time is highly desirable.

In this work, we proposed a lithography-less technique to quantify SOT using the harmonic Hall measurement on continuous thin films. Instead of a conventional Hall cross-device, continuous thin films are directly probed using a customized four-probe arranged in a rhombus geometry. The current is injected into the left–right probes while voltages are measured across the top–bottom probes. The electrical current across the continuous film flows with a non-uniform current distribution and a sharp current density peak along the path of minimal distance as opposed to Hall cross devices, where the current density distribution is minimal and often assumed to be uniform by using narrow voltage probing bars. Even though the current density distribution across continuous films is non-uniform, its distribution profile remains constant across different materials given in a uniform film. Thus, the effective SOT field measured on a thin film can be

corrected by a scaling factor to match a Hall cross-device with uniform current density. The correction factor between the continuous films and Hall cross-device was experimentally quantified and verified across different ferromagnet/heavy metal (FM/HM) structures.

A continuous film with a stack of Pt(5)/Co(1.4)/Ti(2) was deposited on the SiO_2 substrate using DC magnetron sputtering. To determine how the four-probe measured SOT can be corrected to align with that measured in the conventional Hall cross-device, a control sample of Hall cross devices with dimension $5 \times 20\ \mu m$ was fabricated, and the SOT is quantified by the conventional harmonic method.[8,14–16] The continuous film and the Hall cross-device of Ti(2)/Pt(5)/Co(1.4)/Ta(5) were fabricated to validate the difference between four-probe measured SOT in the continuous film and the conventional harmonic in Hall cross-device. These four-probe are directly probing on the surface of the continuous film; hence, this film should have a metallic capping in order for the current to distribute across the structure. Here, we are quantifying the Hall voltage in the continuous film; therefore, a pair of probes for current injection and a pair for reading voltage are required. The voltage probes are located along the perpendicular bisector between the current probes to minimize error due to mechanical movement. A customized four-probe arranged in a rhombus geometry with diagonals of $4 \times 8\ mm^2$ was built. The four probes made of BeCu were used to ensure minimal response under magnetic fields during measurement. The current probe (I_s, I_g) and voltage probe (V_s, V_g) are fixed in the shorter (4 mm) and longer (8 mm) diagonal of the rhombus, respectively, as shown in Fig. 1(a).

Finite-element method (FEM) simulation using COMSOL was performed to quantify the current shunting effects of the voltage probes. Figure 1(b) shows the derived current distribution across different distances of voltage probes, and significant shunting is present for voltage probe distances ≤ 4 mm. Based on the FEM simulation results, the voltage probe separation of 8 mm was preferred where the shunting effect is less than 6% of the total injected current density. To gain a deeper understanding of the current density distribution in the Hall cross-device and continuous film, FEM was also performed on the Hall cross-device with a dimension of $5 \times 20\ \mu m$ and a continuous film dimension of $4\ mm \times 8\ mm^2$. Figures 2(a) and 2(b) show the FEM simulation results of the surface current between the Hall cross-device and continuous film, respectively. The current distribution along the Hall cross-device is almost uniform due to boundary constraints, whereas a diverging current is apparent in the continuous film due to the unconstrained boundary. Therefore, square-like and Gaussian-like current distributions across the characterization width were obtained in the Hall device and continuous film, respectively, as illustrated in Fig. 2(c). From the current distribution profile obtained from the finite element simulation, we will discuss the correlation of H_{DL} between the Hall cross-device and continuous film. The typical Hall voltage in a strong static field is given by $V_H = \int J(y) R_A dA$, where $J(y)$ is the function of current density distribution dependent on spatial position, y and the anamlous Hall resistance, R_A. The total Hall voltage can be expressed as the summation of the zeroth-order harmonic Hall voltage, V_0, the first harmonic Hall voltage, V_ω, and second harmonic Hall voltages, $V_{2\omega}$[8,9,17–19]

$$V_H = V_0 + V_\omega \sin \omega t + V_{2\omega} \cos 2\omega t, \tag{1}$$

$$V_\omega = \frac{1}{2} \Delta I R_A \cos\theta, \quad V_\omega = \frac{1}{2} R_A \cos\theta \int J(y) dA, \tag{2}$$

$$V_{2\omega} = -\frac{1}{2} (\Delta I R_A \sin\theta) \Delta\theta, \quad V_{2\omega} = -\frac{1}{2} R_A \sin\theta \int J(y) \Delta\theta dA, \tag{3}$$

where $\Delta\theta$ is the change in the polar magnetization angle from its equilibrium due to the current-induced SOT. This $\Delta\theta$ is proportional to I, which yields

$$V_{2\omega} = \frac{1}{2} k_1 R_A \sin\theta \int |J(y)|^2 dA, \tag{4}$$

where $k_1 = \Delta\theta / J$ is a coefficient accounting for the linear scaling of $\Delta\theta$ to current density. Utilizing V_ω and $V_{2\omega}$, the damping-like field, H_{DL} can be defined by the following relations:[8,13,20,21]

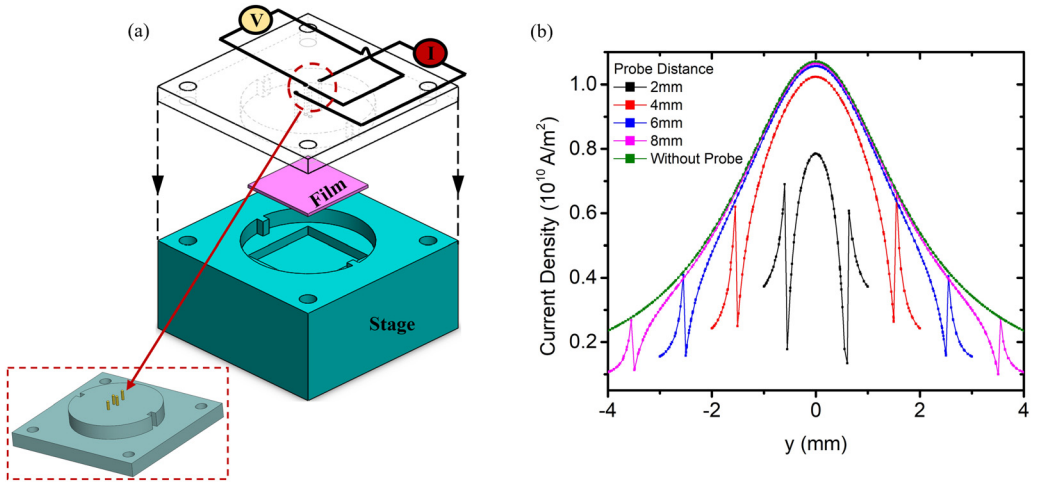

FIG. 1. (a) Schematic setup for four-probe harmonic Hall measurement, where the current probe distance and voltage probe distance are 4 and 8 mm, respectively. (b) Current distribution due to shunting effects across the different voltage probe distances, d = 2, 4, 6, and 8 mm at a current probe distance of 8 mm.

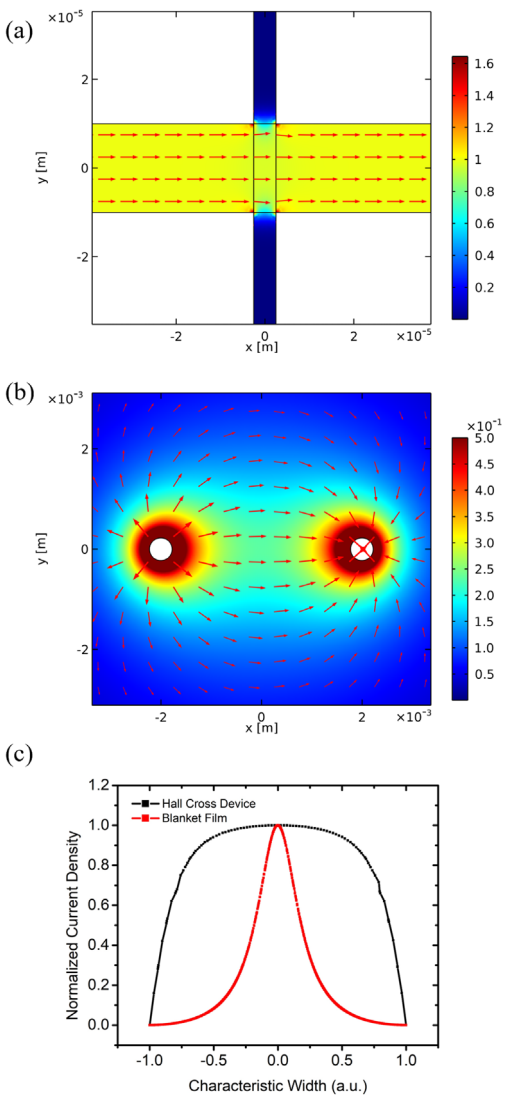

FIG. 2. (a) Current distribution in a 20 × 5 μ m^2 Hall cross device. (b) Current distribution in a continuous thin film at a current probe distance of 8 mm. (c) Current distribution profile of the Hall cross device and continuous film.

$$H_{DL} = -2\left(\frac{\partial V_{2\omega}}{\partial H} \Big/ \frac{\partial^2 V_{\omega}}{\partial H^2}\right), \tag{5}$$

$$H_{DL} = -2\left(\frac{\partial}{\partial H}\left(\frac{1}{2}k_1 R_A \sin\theta \int |J(y)|^2 dA\right) \Big/ \frac{\partial^2}{\partial H^2}\left(\frac{1}{2}R_A \cos\theta \int J(y) dA\right)\right),$$

$$H_{DL} = k_2 \frac{\int |J(y)|^2 dA}{\int J(y) dA}, \tag{6}$$

where k_2 is a linear scaling of H_{DL} per unit current density. To evaluate a correction factor, β_{SOT}, a correlating H_{DL} term between the Hall cross-device and continuous film, β_{SOT} is defined as

$$\beta_{SOT} = k_3 \frac{H_{DL,Blanket} \Big/ \int J_{Blanket}(y) dy}{H_{DL,Device} \Big/ \int J_{Device}(y) dy} = k_3 \frac{\chi_{DL,Blanket}}{\chi_{DL,Device}}$$

$$= k_3 \frac{\int |g_{Blanket}(y)|^2 dy}{\int g_{Blanket}(y) dy}, \tag{7}$$

where χ_{DL} is the damping-like efficiency and k_3 is a linear scaling factor between J_{avg} and J_0. J_{avg} is the average current density across the whole structure given by $J_{avg} = \frac{I}{t\,w}$, where I is the current, t is the film thickness, and w is the distance between the voltage probes. J_0 is the peak current density across the continuous film, and $g(y)$ is the current distribution in the film. Therefore, the SOT in the Hall cross-device is scalable to SOT in the continuous film by a single constant, β_{SOT}. As shown in (7), this β_{SOT} is independent of R_A, indicating that β_{SOT} is constant for any given materials in an identical four-probe geometry setup.

Aside from the difference in using a continuous film instead of a Hall cross-device, the four-probe harmonic Hall measurement uses the setup and procedure as the conventional harmonic Hall measurement. The four-probe setup was placed in an in-plane (IP) sweeping magnetic field, H_x of ±2780 Oe and a fixed out-of-plane (OOP) magnetic field, H_z of 800 Oe. Since the area of measurement in the continuous film is significantly larger than the Hall cross-device, a H_Z is required to ensure the perpendicular magnetic anisotropy (PMA) continuous film remains saturated without domain nucleation within the effective measurement area.[22,23] AC was injected through the continuous film in a longitudinal scheme with respect to H_x. The effective area is defined by the distance between the voltage probe and thin film thickness. The first and second harmonic Hall voltages, V_ω and $V_{2\omega}$ were then measured with different current densities ranging from $J_c = 4.0 \times 10^8$ to 6.0×10^8 A/m^2. The damping-like field, H_{DL} was then extracted from V_ω and $V_{2\omega}$ using (5). Figures 3(a) and 3(b) show the V_ω and $V_{2\omega}$ signals with respect to H_x under a range of current densities. To prevent any Joule heating due to the high current injected, the continuous film was let to cooldown for 120 s before each current density measurement. The H_{DL} is then extracted by using (5), and the damping-like efficiency, χ_{DL} is obtained by fitting H_{DL} against J_c as shown in Fig. 3(c). The values shown in Fig. 3(c) are averaged over five measurements, and the error bar is determined by the standard deviation across all five measurements. To improve the stability of the physical setup, particularly under high magnetic fields, non-ferrous pins had been employed. However, the high current required for thin film measurements inevitably introduces setup perturbations that limit the measurement resolution, leading to the error shown in Figs. 3(c) and 3(d). Here, we have obtained the uncorrected four-probe damping-like efficiency, $\chi_{DL,\,Blanket}$ of 532 ± 44 Oe per 10^{10} A/m^2 for the Pt/Co/Ti structure, which is significantly larger than the literature values.[14,24,25] As discussed above, the divergence of the current in the continuous film is not constraint to a boundary, unlike a pattern Hall cross-device. Therefore, a correction factor, β_{SOT} is required to correct $\chi_{DL.\,Blanket}$ to

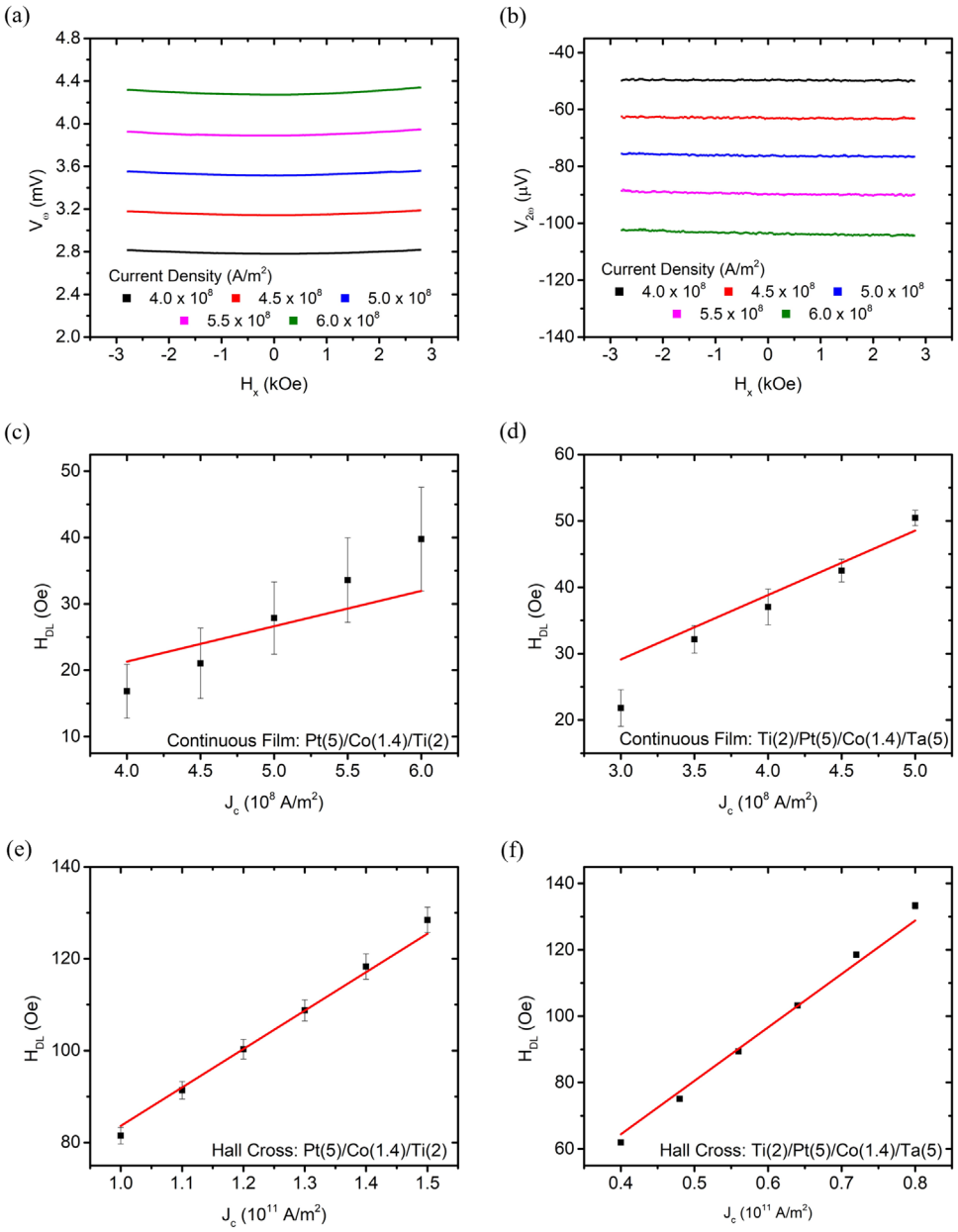

FIG. 3. (a) First harmonic voltage, V_ω and (b) second harmonic voltage, $V_{2\omega}$ in a four-probe harmonic measurement across different ranges of current densities, J_c for Pt/Co/Ti continuous films. (c) and (d) Four-probe results for damping-like field, H_{DL} as a function of J_c for Pt(5)/Co(1.4)/Ti(2) and Ti(2)/Pt(5)/Co(1.4)/Ta(5), respectively. (e) and (f) Damping-like field, H_{DL} as a function of J_c for Pt(5)/Co(1.4)/Ti(2) and Ti(2)/Pt(5)/Co(1.4)/Ta(5) for Hall cross devices.

the damping-like efficiency of device, $\chi_{DL,Device}$. This correction factor, β_{SOT} is experimentally quantified by taking the ratio of χ_{DL} between the continuous film and patterned Hall cross device with the identical Pt/Co/Ti heterostructure. The damping-like efficiency of the device, $\chi_{DL,\,Device}$ was subsequently measured using the harmonic Hall technique and found to be 8.4 Oe per 10^{10} A/m^2 as shown in Fig. 3(e). Thus, $\beta_{SOT} = k_3 \frac{\chi_{DL,Blanket}}{\chi_{DL,Device}} = 63$ is experimentally evaluated. The experiment is repeated with a different heterostructure, Ti(2)/Pt(5)/Co(1.4)/Ta(5) to validate the value of β_{SOT}. Similarly, the uncorrected $\chi_{DL.\,Blanket}$ of the continuous film and $\chi_{DL.\,Device}$ of the Hall cross-device are measured to be 971 ± 30 and 16.1 Oe per 10^{10} A/m^2, respectively, as shown in Figs. 3(d) and 3(f), and thus, $\beta_{SOT} = 60$ is evaluated. Therefore, we can conclude that β_{SOT} is measured to be ∼62. The SOT contribution from the planar Hall resistance is neglected in this work, as it is negligible in comparison to the anomalous Hall resistance in the PMA samples. Note that the value of β_{SOT} remains unaffected by this estimate as it is a ratio of H_{DL} magnitudes between the continuous film and Hall cross-device computed under the same assumptions. Utilizing this value of β_{SOT}, H_{DL} of any ferromagnetic heterostructure can directly be determined without any

lithography process. Apart from the SOT measurement, the four-probe is also applicable in measuring the out-of-plane magnetic hysteresis loop using the anomalous Hall resistance measurement. The anomalous Hall resistance, R_{AHE} of the Pt/Co/Ti structure is measured by applying a sweeping out-of-plane field, H_z of ± 400 Oe concurrently with an AC density, J_c of 1×10^9 and 1×10^{10} A/m^2 to the continuous film and Hall device, respectively. Figure 4(a) shows the ratio between the anomalous Hall resistance, R_{AHE} (Hall cross-device and continuous film) and R_{sat}, where R_{sat} is the magnitude of anomalous Hall resistance of the Hall device. The $R_{AHE,device}$ is found to be approximately 20 times larger than $R_{AHE,\,blanket}$ due to the non-uniform current distribution. The correction factor in anomalous Hall effect (AHE) measurement should not be compared directly with SOT measurement, because in AHE measurement, an OOP field is applied to saturate the magnetization in $\pm m_z$. Since the magnetization is always in $\boldsymbol{M} = \pm(0, 0, m_z)$, hence $\Delta m = 0$. Therefore, AHE measurement is linearly proportional to the profile of the non-uniform current distribution shown in Fig. 4(b). On the contrary, in the harmonic Hall measurement for SOT, we are measuring ΔR_H, which is dependent on the changed in magnetization $\Delta m(x, y, z)$. Due to SOT, $\Delta m(x, y, z)$ will be perturbed following the current density distribution; hence, the SOT measurement is directly proportional to the square of the profile of the non-uniform current distribution, which results in different correction factors obtained between AHE and SOT measurement.

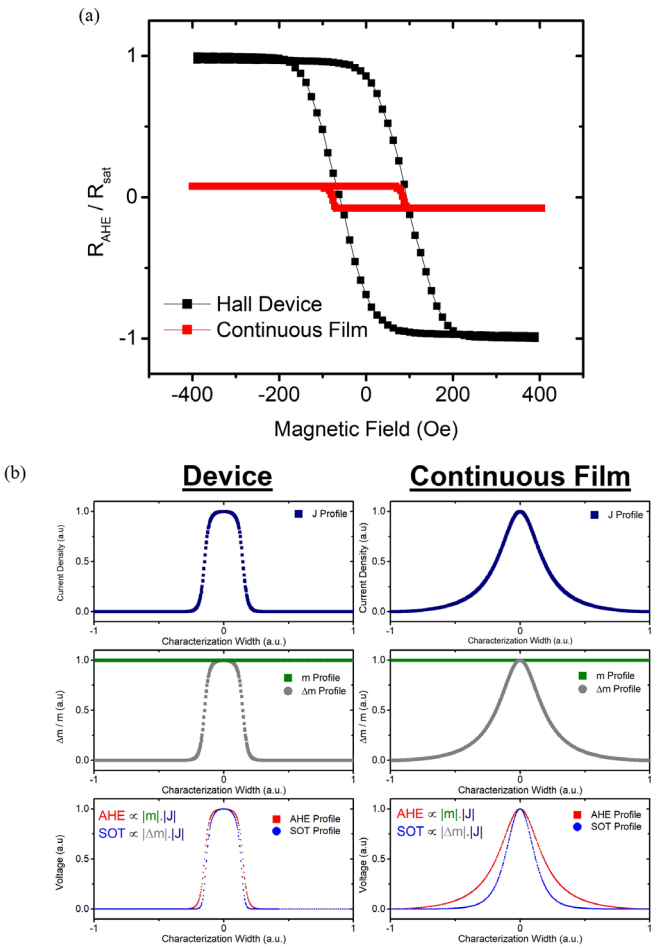

FIG. 4. (a) Ratio between anomalous Hall resistance, R_{AHE} (Hall cross device and continuous film) and R_{sat}, where R_{sat} is the magnitude of anomalous Hall resistance of the Hall device. (b) Comparison between the Hall cross-device and continuous film for the current density profile (first row), m and Δm profile (second row), and AHE/SOT profile (third row).

In conclusion, we have shown a measurement technique using four-probe to directly determine the SOT of the heterostructure without lithography processes, which cost additional resources and time. The H_{DL} of the continuous films were characterized using the harmonic Hall technique by accounting for the divergent current distribution using a constant scaling factor. This correction factor of 62 is experimentally quantified by taking the ratio of the H_{DL} between continuous films and Hall devices. The proposed technique is a cost-effective characterization of SOT efficiency, which is akin to the current in-plane technique that is currently widely used in the industry for obtaining tunneling magnetoresistance from thin-film stacks without any lithography steps.

We thank W. L. Gan for the discussion that led to this work. This work was supported by Research Innovation and Enterprise 2020 Agency for Science, Technology and Research Advanced Manufacturing and Engineering Industrial Alignment Fund - Industry Collaboration Projects (RIE 2020 ASTAR AME IAF-ICP) (Grant No. I1801E0030) and EDB-IPP: Economic Development Board - Industrial Postgraduate Program (Grant No. RCA-2019-1376).

AUTHOR DECLARATIONS

Conflict of Interest

The authors have no conflicts to disclose.

Author Contributions

Han Yin Poh: Conceptualization (lead); Data curation (lead); Formal analysis (lead); Investigation (lead); Methodology (lead); Project administration (lead); Resources (lead); Software (lead); Validation (lead); Visualization (lead); Writing – original draft (lead); Writing – review and editing (lead). **Calvin Ching Ian Ang:** Conceptualization (supporting); Formal analysis (equal); Investigation (equal); Visualization (supporting); Writing – original draft (supporting); Writing – review and editing (supporting). **Tianli Jin:** Methodology (equal); Writing – original draft (supporting); Writing – review and editing (supporting). **Funan Tan:** Conceptualization (supporting); Methodology (supporting); Writing – original draft (supporting); Writing – review and editing (supporting). **Gerard Joseph Lim:** Methodology (supporting); Resources (equal); Writing – original draft (supporting); Writing – review and editing (supporting). **Shuo Wu:** Methodology (supporting); Resources (supporting). **Francis Poh:** Funding acquisition (supporting); Resources (supporting); Supervision (supporting). **Wen Siang Lew:** Funding acquisition (lead); Investigation (supporting); Supervision (equal); Writing – original draft (supporting); Writing – review and editing (supporting).

DATA AVAILABILITY

The data that support the findings of this study are available from the corresponding author upon reasonable request.

REFERENCES

[1]C. Song, R. Zhang, L. Liao, Y. Zhou, X. Zhou, R. Chen, Y. You, X. Chen, and F. Pan, Prog. Mater. Sci. **118**, 100761 (2021).
[2]X. Qiu, K. Narayanapillai, Y. Wu, P. Deorani, D.-H. Yang, W.-S. Noh, J.-H. Park, K.-J. Lee, H.-W. Lee, and H. Yang, Nat. Nanotechnol. **10**, 333 (2015).
[3]X. Qiu, Z. Shi, W. Fan, S. Zhou, and H. Yang, Adv. Mater. **30**, 1705699 (2018).
[4]M. Jamali, K. Narayanapillai, X. Qiu, L. M. Loong, A. Manchon, and H. Yang, Phys. Rev. Lett. **111**, 246602 (2013).
[5]S. Fukami, C. Zhang, S. DuttaGupta, A. Kurenkov, and H. Ohno, Nat. Mater. **15**, 535 (2016).
[6]H. Y. Poh, C. C. I. Ang, W. L. Gan, G. J. Lim, and W. S. Lew, Phys. Rev. B **104**, 224416 (2021).
[7]H. Yang, H. Chen, M. Tang, S. Hu, and X. Qiu, Phys. Rev. B **102**, 24427 (2020).
[8]M. Hayashi, J. Kim, M. Yamanouchi, and H. Ohno, Phys. Rev. B **89**, 144425 (2014).
[9]E.-S. Park, D.-K. Lee, B.-C. Min, and K.-J. Lee, Phys. Rev. B **100**, 214438 (2019).
[10]L. Liu, T. Moriyama, D. C. Ralph, and R. A. Buhrman, Phys. Rev. Lett. **106**, 36601 (2011).
[11]C.-F. Pai, M. Mann, A. J. Tan, and G. S. D. Beach, Phys. Rev. B **93**, 144409 (2016).
[12]T. Jin, G. J. Lim, H. Y. Poh, S. Wu, F. Tan, and W. S. Lew, ACS Appl. Mater. Interfaces **14**, 9781 (2022).
[13]F. Luo, S. Goolaup, W. C. Law, S. Li, F. Tan, C. Engel, T. Zhou, and W. S. Lew, Phys. Rev. B **95**, 174415 (2017).
[14]T. Jin, W. C. Law, D. Kumar, F. Luo, Q. Y. Wong, G. J. Lim, X. Wang, W. S. Lew, and S. N. Piramanayagam, APL Mater. **8**, 111111 (2020).
[15]S. C. Baek, V. P. Amin, Y.-W. Oh, G. Go, S.-J. Lee, G.-H. Lee, K.-J. Kim, M. D. Stiles, B.-G. Park, and K.-J. Lee, Nat. Mater. **17**, 509 (2018).
[16]L. You, O. J. Lee, D. Bhowmik, D. Labanowski, J. Hong, J. Bokor, and S. Salahuddin, Proc. Natl. Acad. Sci. U. S. A. **112**, 10310 (2015).
[17]B. Han, B. Wang, Z. Yan, T. Wang, D. Yang, X. Fan, Y. Wang, and J. Cao, Phys. Rev. Appl. **13**, 14065 (2020).
[18]L. Neumann and M. Meinert, AIP Adv. **8**, 95320 (2018).
[19]C. Engel, S. Goolaup, F. Luo, and W. S. Lew, IEEE Trans. Magn. **53**, 1400604 (2017).
[20]C. Engel, S. Goolaup, F. Luo, and W. S. Lew, Phys. Rev. B **96**, 054407 (2017).
[21]Y. Du, R. Thompson, M. Kohda, and J. Nitta, AIP Adv. **11**, 25033 (2021).
[22]J.-S. Kim, Y.-S. Nam, D.-Y. Kim, Y.-K. Park, M.-H. Park, and S.-B. Choe, AIP Adv. **8**, 56009 (2018).
[23]Q. Y. Wong, C. Murapaka, W. C. Law, W. L. Gan, G. J. Lim, and W. S. Lew, Phys. Rev. Appl. **11**, 24057 (2019).
[24]L. Zhu, D. C. Ralph, and R. A. Buhrman, Phys. Rev. Lett. **122**, 77201 (2019).
[25]H. Xie, J. Yuan, Z. Luo, Y. Yang, and Y. Wu, Sci. Rep. **9**, 17254 (2019).